Interactive comment on "Vertical distribution of chlorophyll in dynamically distinct regions of the southern Bay of Bengal" by Venugopal Thushara et al.

Reply to comments by Referee 1

(Referee's comments are given in blue and the response to comments are in black.)

Based on an observational campaign in the southern Bay of Bengal authors have tried to document the bio-physical interactions, particularly for the evolution of surface/subsurface chlorophyll blooms, in this region during the summer monsoon. They have also used an OGCM to explain the dynamical processes relating to the nitrate limitations for the chl concentration. Considering the data sparsity in the Bay of Bangal, particularly for the biogeochemical data, this manuscript certainly contributes to enhance the existing literature of this region. However, I often find statements made in this manuscript are not well supported by the figures. Below, I have listed some of them.

The referee has made a constructive review on the manuscript which has helped to improve the analysis and presentation of results. We thank the referee for the comments and we have addressed each of them below.

Also, I have serious doubt about the application of the model, particularly because spin-up time for the biogeochemical model is only 10 years, which is way too small for the nutrient levels to be stabilized. I believe, for such a basin scale TOPAZ, a minimum 30-50 years of spin-up is needed to stabilize the climatological nutrient levels, which will ultimately determine the surface chl concentration. Authors may plot the climatological simulation for the subsurface nitrate to see if that is stabilized. However, as this manuscript described the processes for a month long only and therefore, the results presented here might be unaffected by the slow drift in the nutrient levels of the model during the initial spin-up. But even then, a proper spin-up would be a good choice. Further, what about using open boundary conditions for the biogeochemical variables?

Thanks to the referee for the suggestion. The time evolution of biological variables obtained from the ecosystem model shows that the spin up period of 10 years is fairly sufficient to address the processes that we are curretly looking at. Time series of chlorophyll and nitrate at different depth ranges in the southern Bay of Bengal from the

model spin up is shown in Fig. R1. Chlorophyll and nutrient levels show a stable annual cycle after 5-7 years of the spin up. Any model drift in the deep ocean circulation or nutrients is unlikely to affect the upper ocean bloom dynamics in the given time scale of interest. For the biogeochemical variables, no-flux condition has been applied at the open boundaries in the south and east. Open boundaries in the present model configuration are away from the study region and these boundaries have little impact on the model results for the timescale of our interest.

Page15, line 7-10: "The hydrodynamics of the region suggests that the triggering mechanism for bloom generation is open ocean Ekman pumping forced by positive wind stress curl (Vinayachandran et al., 2004; Wijesekera et al., 2016a), favouring vertical transport of nutrients to the surface sunlit layers."

The authors relied too much on referencing. It is not difficult to calculate Ekman Pumping for the specific period. Authors are encouraged show that indeed the Ekman pumping is the primary driver. What about instability? This region exhibits one of the strongest barotropic/baroclinic instability of the north Indian Ocean.

Thanks to the referee for pointing out this. We agree with the referee's comment on processes other than Ekman pumping in controlling the bloom dynamics in the region of the Sri Lanka Dome (SLD). Ekman pumping was calculated using ASCAT winds as shown in Fig. R2. Time series over the location of SG579 shows upwelling tendencies during most of the observational period (Fig. R2a). Pumping velocities peaked to about 2-3 m day^{-1} by mid-June. Time series of minimum SLA shows that SLD attained its peak by the end of June (Fig. R2a), coinciding with the observed bloom at SG579. Ekman pumping remained to be upwelling favourable (0.4-0.7 m day^{-1}) during the period of surface bloom (30 June-02 July), though the magnitudes were relatively weaker. Strong upwelling in the second half of June, prior to the bloom event, is presumed to provide a favourable pre-conditioning by lifting the nitracline towards the surface. (This is explained below using the ecosystem model). Spatial distribution of mean Ekman pumping averaged for the BoBBLE observational period (24 June – 23 July) indicates widespread upwelling in the southern BoB (Fig. R2b).

During the decaying phase of the SLD in July, Ekman pumping velocities were positive, with peak values of about 2 m day^{-1} (Fig. R2a). This indicates that the influence of remote

effects propagating from the eastern boundary of the BoB were dominant during this period (Vinayachandran and Yamagata 1998; Shankar et al., 2002; Wijesekera et al. 2016; Burns et al., 2017; Webber et al., 2018). Time-longitude hovmoller diagram of SLA from AVISO during May-July along 8°N, between 80-100°E is shown in Fig. R3. The decay period of SLD coincides with the arrival of positive SLA anomalies from east, representing the westward propagation of downwelling Rossby waves (Webber et al., 2018). This shows that, despite the positive Ekman pumping, remote forcings from the east contributed to the weakening of the SLD. The dynamics of the BoB is also characterised by instability effects associated with barotropic and baroclinic energy conversions (Vinayachandran and Yamagata, 1998; Kurien et al., 2010; Cheng et al., 2017). A complete energy analysis to examine the role of instability is beyond the scope of this paper. As far as the surface bloom generation is concerned, the proximity of nutricline to the surface (as well as the light availability, which will be explained in the following sections) is of primary concern. Hence we relied on the ecosystem model to identify the dominant forcing controlling the vertical displacement of nitracline.

Modelled SLD peaked on 28 June, two days prior to the observed peak. The developing phase of simulated SLD (14-28 July) was characterised by the shoaling of nitracline. The shoaling rate of nitracline increased to about 1.0 m day^{-1} by mid-June and closely followed the Ekman pumping velocities (Fig. R4). This shows that the vertical supply of nutrients to the surface layers during the developing phase of the SLD can be largely attributed to Ekman pumping. During the peak phase of SLD, both Ekman pumping velocities and nitracline shoaling rates weakened. However, the larger shoaling rates during the preceeding week indicate a favourable pre-conditioning for bloom generation during the peak phase of SLD. Later, during the decaying phase of the SLD in July, Ekman pumping gradually increased. However, the corresponding nitracline variability (with deepening tendencies) was not consistent with the pumping velocities, indicating the effect of remote forcings. These additional explanations will be added in Section 3.2.1 of the manuscript and Figures R2, R3 and R4 will be included.

Page 15, line no. 15: "The decay of surface bloom after 02 July (Fig. 5) followed the weakening of the dome (Fig. 3)." Not vary clear

Time series of minimum SLA in the region of the dome is shown in Fig. R2a. Sea level

anomalies decreased to about -0.3 m on 30 June. Intensification of SLD coincided with the observed surface bloom at SG579. The dome weakened afterwards as indicated by the weakening of negative SLA. The bloom decay after 02 July followed the weakening of the dome. This will be clarified in Section 3.2.1 of the manuscript and Fig. R2 will be included.

Page 15, lines 17-21: "CTD observations within the dome until 29 June, when the ship was at TSW, show that the subsurface chlorophyll concentrations were weak (< 0.5 mg m −3) just before the surface bloom event (Fig. 4e). This indicates that the vertical redistribution of subsurface phytoplankton does not have significant contribution in enhancing the surface chlorophyll. The generation of surface blooms is presumed to be dominantly controlled by the vertical transport of subsurface nutrients to the euphotic zone."

The mixed layer in SG579 does not seems shallowed considerably during the initial phase, but the chl concentration enhanced significantly in the mixed layer. The clear sky might be the major factor for this surface bloom as the authors said that the monsoon was active and therefore had considerable cloud cover in the previous week. It is possible that as the sky became clear it enhance the available light and thus marked by enhanced Chl. However, as the surface nutrients get consumed in few days the Chl concentration decreases again in spite of the persistence clear sky. How, authors can discard this possibility?

We thank the referee for pointing out this possibility. Photosynthetically available radiation (PAR) from MODIS/VIIRS merged product along 8° N from June to July is shown in Fig. R5. The study region was under the influence of an active phase of the monsoon until the third week of June. This indicates light limitation on phytoplankton growth during this period. The active phase was followed by a convectively suppressed phase by the last week of June, one week prior to the glider deployment. In the region of SLD, PAR levels increased from about 12 E m^{-2} day^{-1} on 22 June to 50 E m^{-2} day^{-1} on 26 June. This shows that the transition from active to supressed phase favoured enhanced light availability for bloom generation. The glider data sampling began on 30 June, after the commencement of the suppressed phase and coinciding with the peak phase of the SLD. This restricts the identification of the relative importance of light and nutrient limitations on the generation of blooms at SG579. It may be noted that high radiation levels persisted till

mid-July, however, the surface layers exhibited oligotrophic conditions after the bloom decay. Surface chlorophyll dropped to levels below 0.1 mg m^{-3} after 02 July (Fig 4a in the manuscript). This implies nutrient depletion in the surface layers resulting from phytoplankton consumption during the bloom event. The above details will be included in Section 3.2.1 of the manuscript. The shoaling of MLD is not so evident in the glider data, probably because the sampling period of SG579 starts on 30 June, when the SLD was already at its peak (Fig. R2a).

Page 16, lines 13-15: "Subsequent deepening of the mixed layer (~70 m, Fig. 4d) suggests the role of mixing and entrainment in triggering the surface blooms."
What happens after 7th July when the MLD shallowed again in spite of increased wind speed? This does not explain authors hypothesis that the MLD deepens due to increased winds.

Mixed layer shoaling after 07 July, despite the increase in wind speed, can be attributed to surface freshening. Surface salinity decreased by about 0.8 psu from 07 July to 10 July, inducing strong near-surface stratification (Fig. 6 in the manuscript). The resultant shoaling of mixed layer and the barrier layer formation (Fig. 7 in the manuscript) reveal the dominant role of freshwater over wind forcing in controlling the near-surface stratification and hence the surface blooms.

Deepening of mixed layer on 06 July occured between two freshening events; the first during 04-05 July and the second during 07-10 July (Fig. 6 in the manuscript). Surface salinity stratification was relatively weaker in between these events, providing conditions favourable for wind induced mixing. Taking into account the dynamic nature of the region, any impact of lateral transport of salinity on mixed layer deepening cannot be ignored. The quantification of lateral transport, however, is not feasible without estimates of advection and hence is outside the scope of the paper.

"The decay period of the bloom (08–10 July) coincided with the development of a freshening event. Surface salinity decreased by about 0.8 psu from 06 July to 10 July (Fig. 6) and the corresponding decrease in surface chlorophyll was about 0.27 mg m −3 (Fig. 5)."

The decrease of salinity during 6-10 July is of same order as seen during 4-5 July. This is

only due to the fact that MLD shallows again and thereby inhibits the subsurface mixing of salinity. It may not be linked with lateral advection of fresh water and more to do with dynamics behind deepening of MLD during 5-7 July, which is not quite explained by the authors.

Later, in Figure 7 authors nicely explained the formation of barrier layer which inhibits surface Chl. However, yet to convincingly explain why MLD deepens during 6-7 July. It may also help to extend the Figure 7 from 3rd July to see the barrier layer evolution.

The decrease in surface salinity cannot be completely attributed to mixed layer shoaling and inhibition of subsurface mixing of salinity. In the absence of an external freshwater source, mixed layer shoaling will not cause any further freshening in the surface layers as observed in the glider data. Since there was no local precipitation, the dominant mechanism which leads to surface freshening is presumed to be lateral advection. Impact of surface freshening on MLD and the barrier layer formation is evident from the profiles before and after the freshening event (Fig. 7 in the manuscript). Inhibition of mixing will finally limit the availability of nutrients in the surface layers and hence the surface bloom decays. Note that the shoaling of mixed layer occurs slightly later at the CTD location (Fig. 4e) and the surface bloom persists for longer here.

Figure 7 has been modifed by including selected daily mean profiles starting from 03 July till 10 July from SG620 (Fig. R6a-e). The barrier layer formation due to surface freshening can be observed during both the freshening events (Vinayachandran et al., 2018). Initial drop in surface salinity during the freshening events were of the same order (~0.4 psu; 04 July and 07 July in Fig. 6 of the manuscript). However, the first event was relatively shorter (04-05 July) and the second event lasted for a longer time period (07-10 July). Inhibition of surface blooms and the intensification of the DCM in the presence of surface salinity stratification can be observed during both the freshening events (Fig. R6b and R6d-e). Vertical profiles obtained from CTD at TSE for the same period are given in Figure R6f-j. CTD data shows both the freshening events, the associated development of barrier layers, the resultant decline in surface chlorophyll and the intensification of DCM, consistent with the glider observations (Fig. R6g and R6i-j). Above details and the modified Fig. 7 will be included in the manuscript.

Page 29, line 11: “ Hence NO 3 was preferred over PO 4 and Fe (SiO4 does not limit

growth in TOPAZ)" I think this statement is not true. In TOPAZv1 large phytoplankton limitation term is dependent on Silicate. Please verify.

Thanks to the reviewer for the correction. SiO4 limits the growth of large phytoplankton in the model, but not considered in the case of small phytoplankton and diazotrophs. The text will be modified accordingly.

Figure 14: This figure is very confusing. It would help to overlay the weekly mean currents over the tendency terms. Many a times statements are made on vortices, SMC and its consequences on the NO3 budget, but without showing the mean currents it is very difficult to follow as a reader.

For example, authors said "Along the path of SMC, a clear patch of increased nitrate levels was evident (Fig. 14i), which extended from the southern tip of India up to about 85E. This indicates horizontal advection of coastally upwelled nutrients from the southern coasts of India and Sri Lanka (Fig. 14k) into the southern BoB by the SMC"

To me the NO3 show a negative tendency in the core of the SMC (east of SriLanka) and the positive patch may be along the edges. However, I can not make a concrete conclusions without any information of currents.

Thanks to the reviewer for the suggestion. Weekly mean currents are overlayed over the tendency terms (Fig. R7). Horizontal advection of coastally upwelled nutrients from the southern coasts of India and Sri Lanka can be seen along the path of SMC (Fig. R7i and R7k).

Further, authors claimed that Ekman pumping is the primary mechanism of surface Chl bloom, which I think is not well supported. Also, what about entrainment? At least SG620 show a clear signature of entrainment during 6-7 July.

Observations from SG579, in the region of SLD, shows no significant deepening of mixed layer during the period of surface blooms (Fig. 4a in the manuscript). This indicates that entrainment was relatively weaker here. Ouside the region of SLD, at TSE, SG620 shows deepening of mixed layer by about 20-30 m during 3rd and 6th July. This indicates a significant contribution of entrainment in the vertical supply of nutrients and hence the

surface bloom formation. Quantification of entrainment, however, requires additional information on the vertical gradient of nutrients.

Finally, what will be the effect of Rossby wave radiations from the eastern boundary of the Bay Bengal. Since, 8N is very close to the equatorial region, Rossby waves can travel pretty fast (~20-25 cm/s ?) which means a Rossby wave front can cover about 2 degrees during the observation period and therefore, can implicate the east-west contrast between TSW and TSE.

We thank the referree for the suggestion. Rossby waves propagating from the eastern boundary of the BoB can influence the depth of thermocline (nitracline) and hence the bloom activity. The east-west contrast between TSW and TSE is largely dependent on the spatial extent and strength of SMC and SLD, which is attributed to the combined effect of local as well as remote forcings. Observations of currents and sea level anomalies reveal that the location and intensity of SMC and SLD varied during the observational period (Fig. 3 in the manuscript). Using geostrophic velocities obtained from satellite data, Webber et al. (2018) showed that the SMC moved westward during the BoBBLE observational period. They related the westward shift of SMC to the westward propagation of downwelling Rossby waves from the eastern boundary of the BoB. The strength and spatial extend of SLD also varied accordingly. The decay period of the SLD coincided with the arrival of westward propagating high in sea level anomalies associated with the Rossby wave propagation (Fig. R3). The above explanations will be included in the manuscript.

References

Burns, J. M., B. Subrahmanyam, and V. S. N. Murty, (2017), On the dynamics of the Sri Lanka Dome in the Bay of Bengal, J. Geophys. Res. Oceans, 122, 7737–7750, doi:10.1002/2017JC012986.

Cheng, X., J. P. McCreary, B. Qiu, Y. Qi, and Y. Du, (2017), Intraseasonal-to-semiannual variability of sea-surface height in the astern, equatorial Indian Ocean and southern Bay of Bengal, J. Geophys. Res. Oceans, 122, doi:10.1002/2016JC012662.

Prescilla Kurien, Motoyoshi Ikeda and Vinu K. Valsala, (2010), Mesoscale Variability along the East Coast of India in Spring as Revealed from Satellite Data and OGCM Simulations, Journal of Oceanography, 66, 273–289

Shankar, D., Vinayachandran, P., and Unnikrishnan, A., (2002), The monsoon currents in the north Indian Ocean, Progress in Oceanography, 52, 63–120.

Vinayachandran, P. N. and Yamagata, T., (1998), Monsoon Response of the Sea around Sri Lanka: Generation of Thermal Domes and Anticyclonic Vortices, J. Phys. Oceanogr., 28, 1946–1960.

Vinayachandran, P. N., and Coauthors, (2018), BoBBLE (Bay of Bengal Boundary Layer Experiment): Ocean–atmosphere interaction and its impact on the South Asian monsoon. *Bull. Amer. Meteor. Soc.*,99, 1569–1587, https://doi.org/10.1175/BAMS-D-16-0230.1.

Webber, B. G. M., Matthews, A. J., Vinayachandran, P. N., Neema, C. P., Sanchez-Franks, A., Vijith, V., Amol, P., and Baranowski, D. B., (2018), The dynamics of the Southwest Monsoon current in 2016 from high-resolution in situ observations and models, Journal of Physical Oceanography, 48, 2259-2282.

Wijesekera, H. W., Shroyer, E., Tandon, A., Ravichandran, M., Sengupta, D., Jinadasa, S. U. P., Fernando, H. J. S., Agarwal, N., and Coauthors, (2016), "ASIRI: An Ocean–Atmosphere Initiative for Bay of Bengal", Bull. Am. Meteorol. Soc., 97, 1859–1884, https://doi.org/10.1175/BAMS-D-14-00197.1.

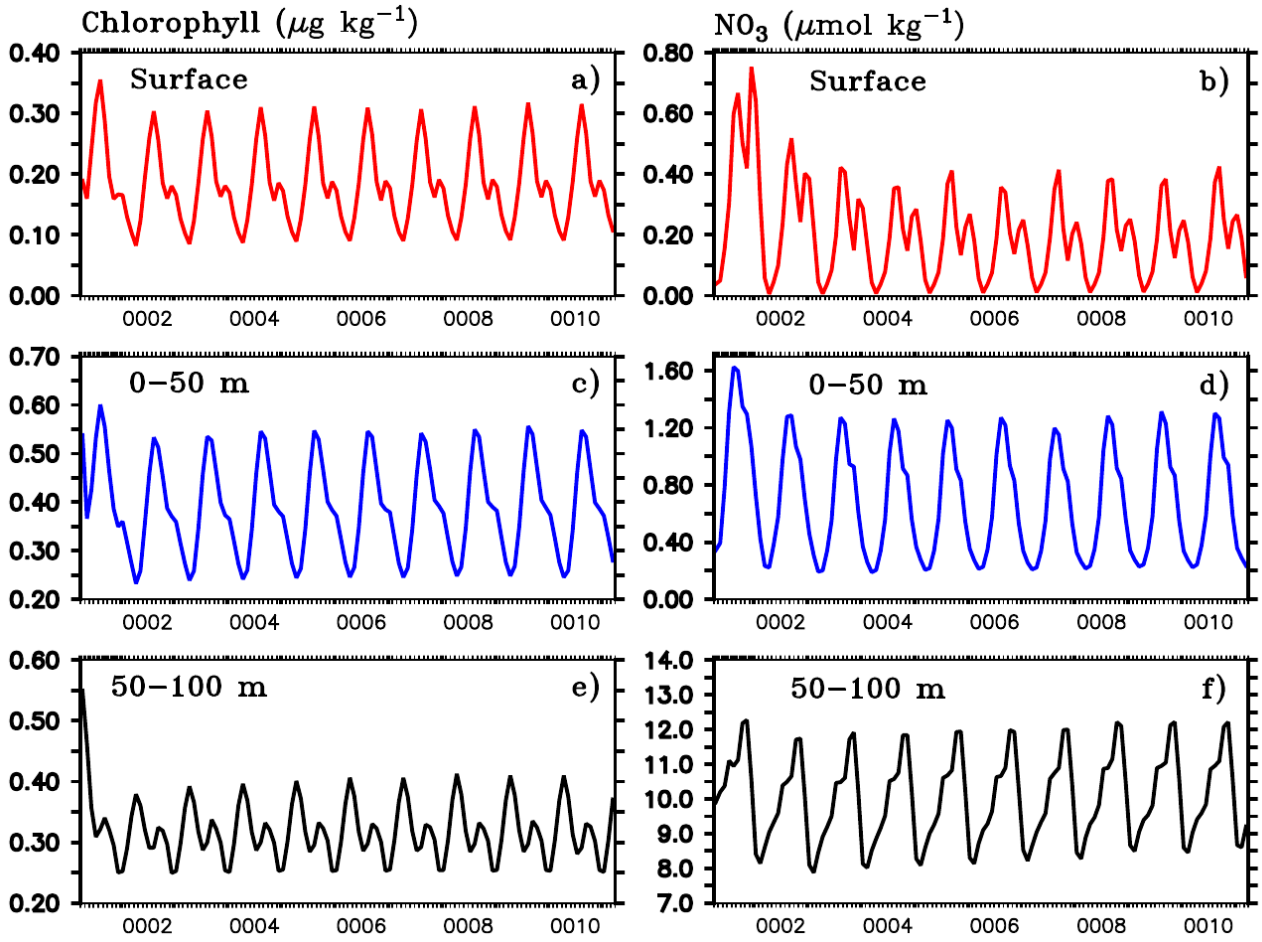

Figure R1. Time evolution of simulated chlorophyll (left panels) and nitrate (right panels) at the surface (top panels), 0-50 m (middle panels) and 50-100 m (bottom panels) for 10 years of the model spin up.

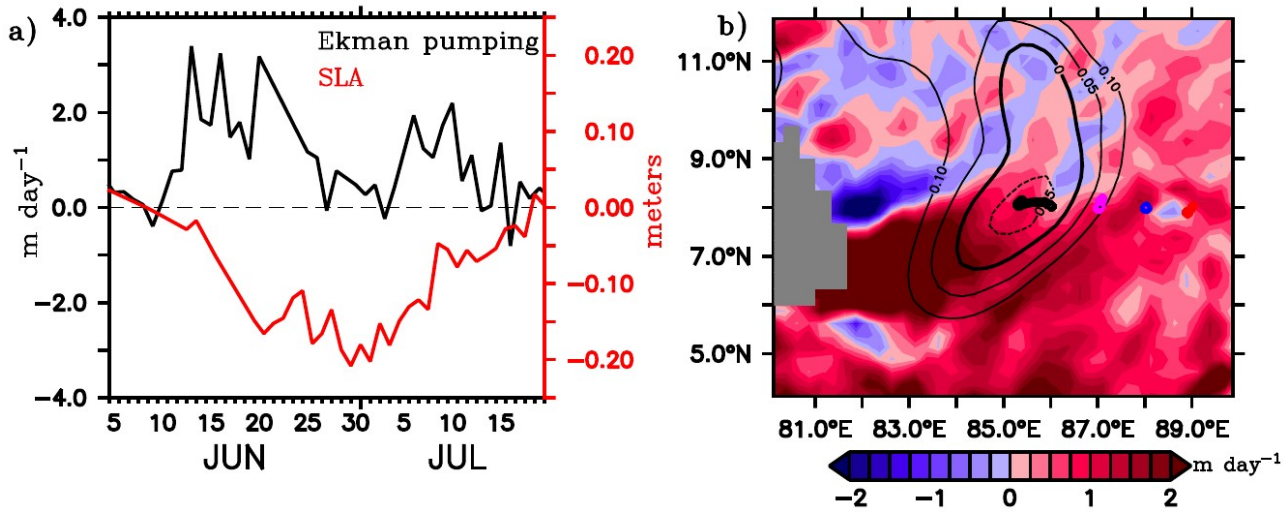

Figure R2. a) Time series of Ekman pumping (m day^{-1}; black) calculated from ASCAT winds around the location of SG579 (85-86° E, 7.5-8.5° N) and the minimum SLA (m; red) in the region of the Sri Lanka Dome (SLD) from 05 June to 20 July. b) Mean Ekman pumping averaged for the BoBBLE observational period (24 June – 23 July) in the southern BoB. Contours of SLA are overlayed.

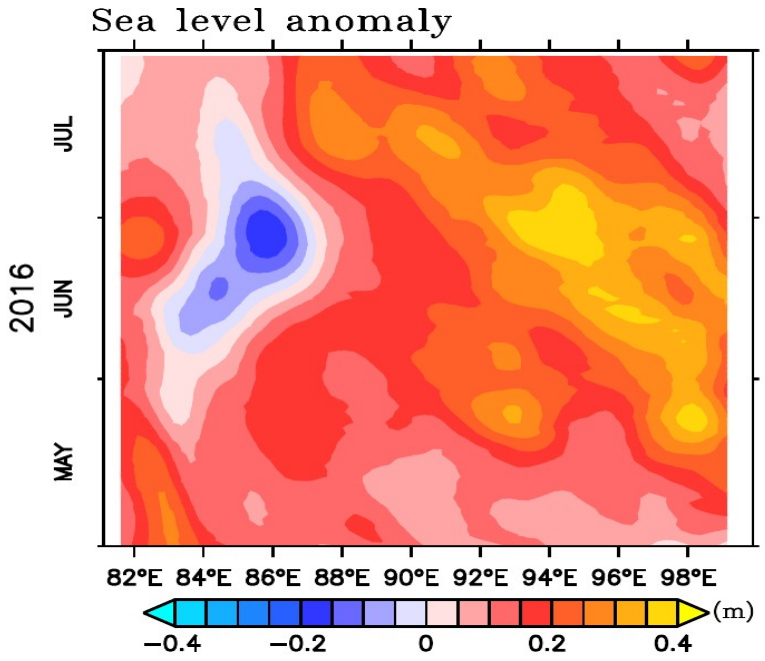

Figure R3. Time-longitude hovmoller diagram of SLA (m) along 8°N between 81-100°E from May to July 2016.

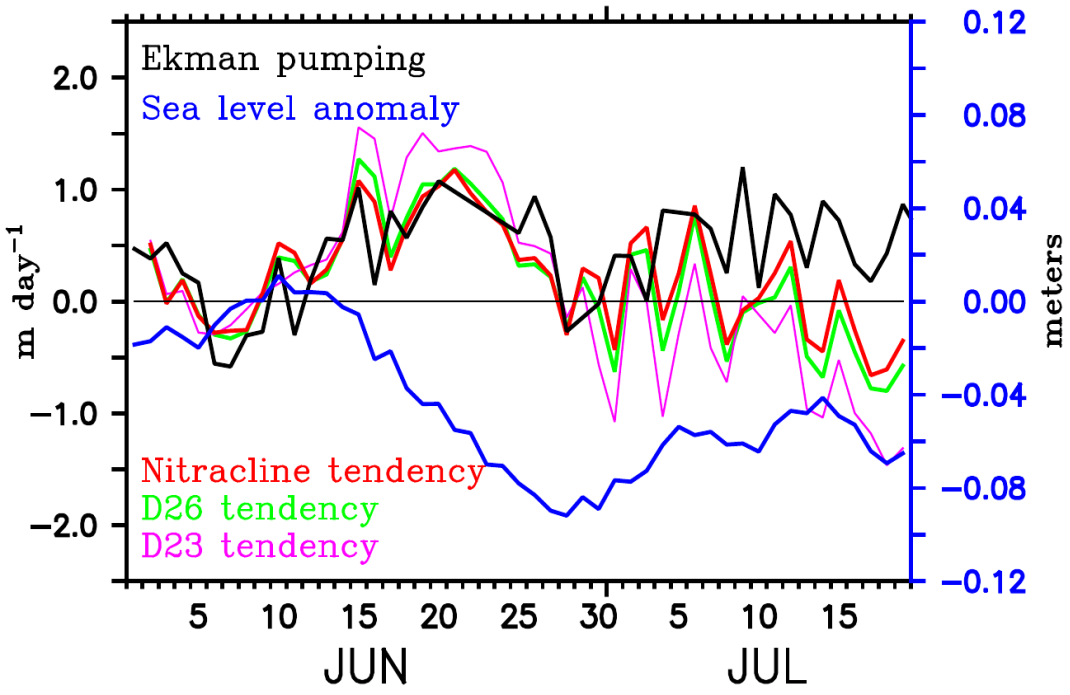

Figure R4. Ekman pumping (m day^{-1}; black) and tendencies of nitracline (m day^{-1}; red), D26 (m day^{-1}; green) and D23 (m day^{-1}; magenta) averaged over the region of the modelled Sri Lanka Dome. Note that the tendency terms are reversed in sign so that positive (negative) values indicate shoaling (deepening). Nitracline is defined as the depth of 2 µmol kg^{-1} nitrate isoline. Minimum sea level anomaly (m; blue) in the region of SLD is overlayed.

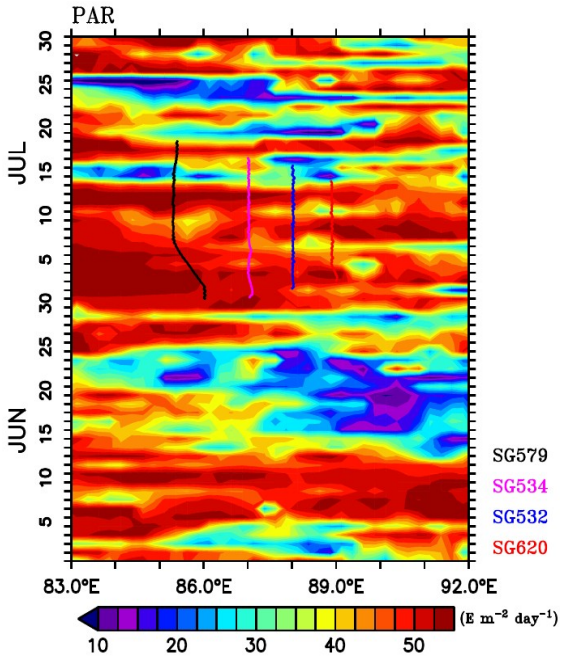

Figure R5: Photosynthetically available radiation (PAR; E m^{-2} day^{-1}) along 8° N, between 83-92° E from June-July, 2016. The glider tracks during the BoBBLE field program are overlayed.

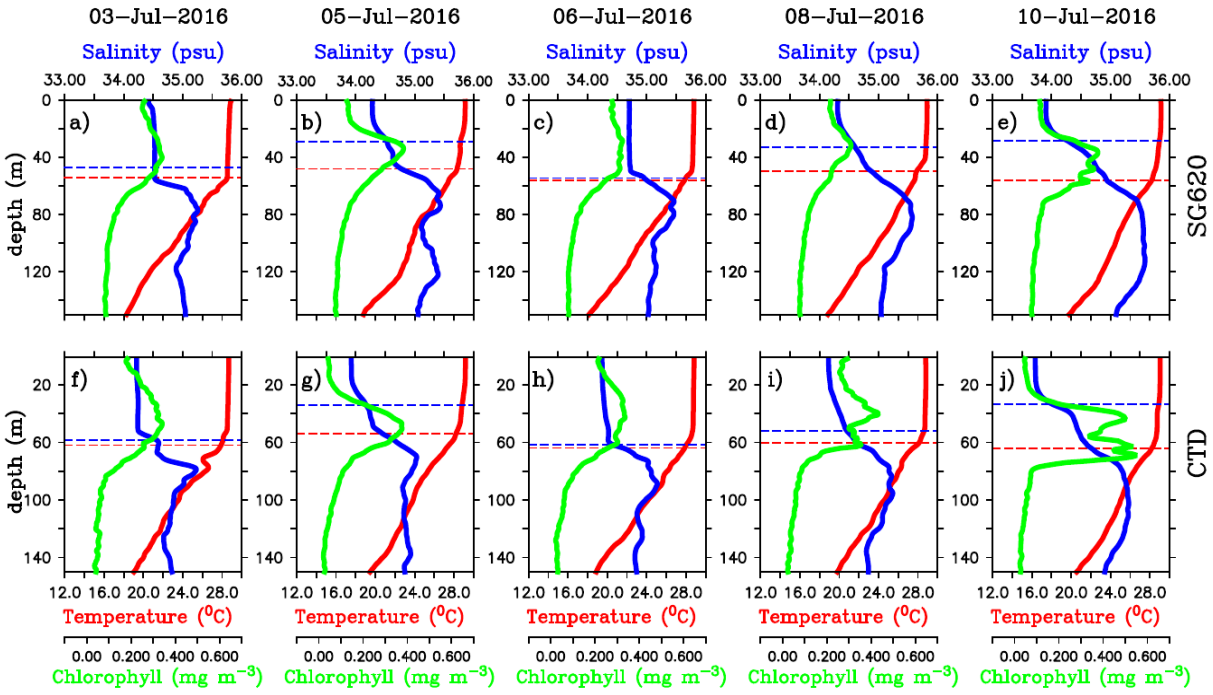

Figure R6. Daily mean vertical profiles of temperature (°C; red), salinity (psu; blue) and chlorophyll (mg m^{-3}; green) from (a-e) SG620 and (f-j) CTD at TSE location for selected days. The blue dashed line indicates the mixed layer depth, which is calculated as the depth where density is equal to the sea surface density plus an increase in density equivalent to 0.8°C. The red dashed line indicates isothermal layer depth (ILD) which is calculated as the depth where the temperature is cooler than SST by 0.8° C. The region between the MLD and ILD represents the barrier layer.

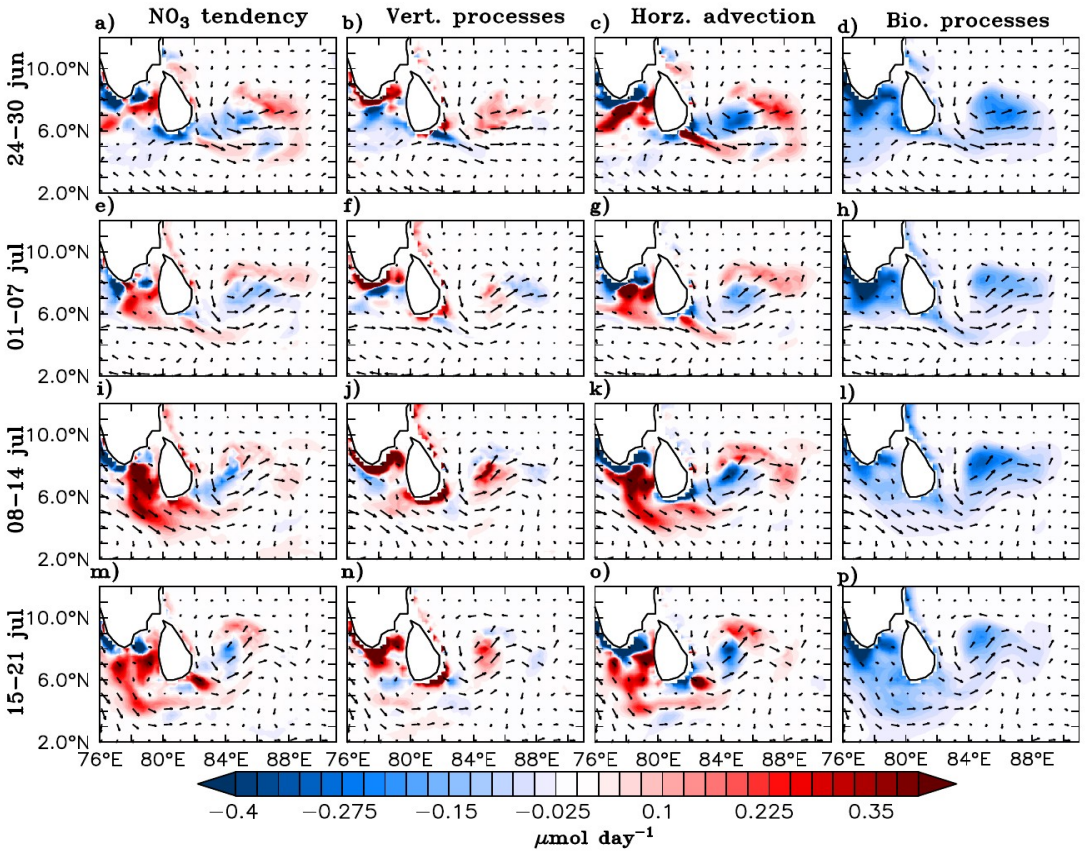

Figure R7. Model nitrate budget averaged over the mixed layer. Nitrate tendency (first column), vertical processes (second column), horizontal advection (third column) and the biological processes (fourth column) in μmol day^{-1} are shown for 7-day averages starting from 24 June to 21 July 2016, marked on the left side of the corresponding panels. Vertical processes include vertical advection and mixing, and biological processes include source (nitrification) and sink (denitrification and uptake by the phytoplankton) terms for the model nitrate. Surface current (ms^{-1}) vectors are overlayed.